

# Experimental Determination of the Discharge Coefficients for Critical Flow through an Axisymmetric Nozzle

S. P. Tang\*

TRW Defense and Space Systems Group, Redondo Beach, Calif.

and

J. B. Fenn†

Yale University, New Haven, Conn.

Discharge coefficients for critical flow nozzles were determined experimentally for hydrogen, helium, nitrogen, and argon over a Reynolds number range from  $10^2$  to  $10^4$ . Above values of about 200, the measured coefficients are in excellent agreement with those predicted by a straightforward application of boundary-layer theory. The results suggest that in many cases experimental calibration of metering nozzles might be avoided.

## Nomenclature

$C_D$	= discharge coefficient $\dot{m}/\dot{m}_{is}$
$C_p$	= specific heat at constant pressure
$D$	= nozzle throat diameter
$\dot{m}$	= actual mass flow rate
$\dot{m}_{is}$	= isentropic mass flow rate
$p$	= pressure
$Pr$	= Prandtl number
$r_c$	= "radius of curvature" of the nozzle wall at the throat
$r_t$	= nozzle throat radius
$Re_D^*$	= Reynolds number based on nozzle throat diameter
$Re_D^*$	= see Eq. (2)
$T$	= temperature
$u$	= velocity component parallel to the wall
$z$	= distance along nozzle axis of symmetry
$\gamma$	= ratio of specific heats
$\delta^*$	= displacement thickness of the boundary layer
$\rho$	= mass density
$\mu$	= absolute viscosity
$\beta$	= pressure-gradient parameter
$\lambda$	= mean free path

## Subscripts

$e$	= local flow outside boundary layer (external)
$0$	= freestream stagnation value
$*$	= sonic condition

## I. Introduction

IN 1969, Tang presented an analysis of the flow through a choked axisymmetric nozzle.<sup>1</sup> The following frequently used assumptions were invoked: 1) the fluid is a perfect gas with constant specific heat; 2) the Prandtl number is unity; 3) the viscosity has a linear dependence upon temperature; and 4) external to the boundary layer, the flow is inviscid and one-dimensional. The analysis is applicable to nozzles having adiabatic walls with contours that can be characterized by the "radius of curvature" at the throat  $r_c$  and a pressure-gradient parameter  $\beta$ , which relates to the streamwise acceleration of the fluid, i.e., the dependence of nozzle cross section upon axial distance. For the case of  $\beta = \infty$ , an exact analytical solution of the equations was possible and gave rise to the

following expression for the discharge coefficient  $C_D$  of the nozzle:

$$C_D = 1 - \left( \frac{\gamma + 1}{2} \right)^{1/2} \left\{ \frac{8[9 - 4(6)^{1/2}]}{3(\gamma + 1)} + \frac{4(6)^{1/2}}{3} \right\} (Re_D^*)^{-1/2} + \frac{2(2)^{1/2}}{3} \frac{(\gamma - 1)(\gamma + 2)}{(\gamma + 1)^{1/2}} (Re_D^*)^{-1} \quad (1)$$

where  $C_D$  is the ratio of actual mass flow to the ideal isentropic value,  $\gamma$  is the specific heat ratio, and  $Re_D^*$  is a modified Reynolds number defined by

$$Re_D^* = (r_c/r_t)^{-1/2} (\rho_e u_e D / \mu_e)_* \quad (2)$$

where  $D$  is the diameter of the nozzle at the throat,  $r_t$  is the throat radius,  $\rho$  is the density,  $u$  is the velocity, and  $\mu$  is the viscosity.<sup>1</sup> Subscript  $e$  indicates freestream values. The asterisk indicates a Mach number of unity, i.e., at the throat.

For values of  $\beta$  other than infinity, an exact analytical solution of the equations was not possible. Numerical solutions for  $\beta = 1$  and  $\beta = 2$  showed that  $C_D$  was very insensitive to the value of  $\beta$ . On the other hand, nozzle contours for different values of  $\beta$  were themselves quite different. These observations imply that the exact solution for  $\beta = \infty$  may be a good approximation for real nozzles having a wide range of contours.

The overall result of the analysis is a relatively simple and straightforward expression [Eq. (1)] for computing the discharge coefficient of an axisymmetric nozzle in critical flow over a range of Reynolds numbers, provided only that the radius of curvature at the throat is finite and known. No empirically adjustable parameters are involved. Experimental confirmation of this result would be theoretically interesting as a test of the many simplifying assumptions that often are used in other contexts. It would be of practical relevance because of the widespread use of small critical nozzles for metering flows, for molecular beam sources, for sampling, for pneumatic thermometry, for microrocket motors, and for other applications. Accordingly, we undertook to put the theory to experimental test. Just because of the widespread use of critical flow nozzles, one might expect that there would be an abundance of data in the literature. As noted in the literature, there are indeed quantities of data but most of them are in the very high Reynolds number range, where discharge coefficients are close to unity.<sup>2-8</sup> Relatively few results are in the range of interest, i.e., Reynolds numbers between  $10^2$  and  $10^4$ . Of those available, many show relatively large scatter. Many do not provide complete details

Received Aug. 24, 1976; revision received Aug. 8, 1977. Copyright © American Institute of Aeronautics and Astronautics, Inc., 1977. All rights reserved.

Index categories: Boundary Layers and Convective Heat Transfer—Laminar; Nozzle and Channel Flow.

\*Systems Group Research Staff.

†Professor, Dept. of Engineering and Applied Science.

on the nozzle shape, i.e., radius of curvature at the throat. Measurements with more than one gas seldom are reported. Consequently, we embarked on a program of measuring discharge coefficients over a range of conditions wide enough to provide an adequate test of the theoretical result presented in Ref. 1. Our data also should be a valuable addition to the progress<sup>9,23</sup> accomplished in recent years.

## II. Experimental Procedures

In principle, the determination of experimental discharge coefficients is straightforward. In practice, to obtain reproducible and accurate flow rate measurements is a tedious procedure that requires painstaking attention to detail. We shall describe our methods and precautions with reference to the schematic representation of our apparatus in Fig. 1.

Upstream of the nozzle, stagnation pressures above 100 Torr were measured with a mercury manometer (Merian Instrument Co., model 20 BA 10). It had a bore of 0.5 in., large enough to eliminate capillarity effects. Below 100 Torr, we used a U-tube "dipstick" manometer. Because its legs were of precision bore tubing (1 in.), it was sufficient to measure changes in meniscus level on only one side by means of a micrometer head (L.S. Starrett Co., No. 63) to which was welded a stainless-steel dipstick with a sharp point. The reference level was obtained when the pressure was the same on both sides. With mercury in the manometer, contact between the meniscus and the dipstick was indicated by closing of an electrical circuit. Reproducibility was within about  $\pm 5 \times 10^{-2}$  Torr over the range of 100 Torr. With low-vapor-pressure oil as the working fluid, contact between the meniscus and the dipstick point gave rise to a readily observable capillary "jump" at the instant of contact. In this case, reproducibility was within about  $\pm 3 \times 10^{-3}$  Torr, and the range was about 7 Torr. The pressure on the reference leg of the manometer was maintained with a mechanical vacuum pump at less than 25 m Torr, as indicated by a thermocouple gage. It was thus negligible in all of our measurements and could be taken as zero. The pressure downstream of the nozzle was monitored with a small absolute mercury manometer. Pressure ratios across the nozzle were always greater than 9, well above the value necessary to insure critical flow. The pressure ratio was maintained by a mechanical vacuum pump (Welch Scientific Company, model 1397). The exhaust flow from the pump was passed through an oil vapor trap comprising a bed of molecular sieve granules and then into a calibrated volumetric flow meter operating at local atmospheric pressure as determined by a mercury-in-glass barometer. Except for one set of high-temperature measurements which will be described separately, nozzle stagnation temperature and flow meter operating temperature were determined with calibrated mercury-in-glass thermometers.

Two flow meters were used. Flow rates above about 1.5 cm<sup>3</sup>/s were measured with a liquid-sealed rotating displacement "wet test meter" (Precision Scientific Co., model 63125). It was calibrated by measuring the pressure

decay in a tank exhausting through the meter. The volume of the tank was determined by weighing the amount of water it could contain. In order to eliminate vapor pressure corrections, we used dibutyl phthalate as the working fluid in the meter. Its vapor pressure was always less than  $10^{-2}$  Torr. Flow rates below about 1.5 cm<sup>3</sup>/s were measured by displacing dibutyl phthalate from an inverted burette whose volume was calibrated with water by weighing. All time intervals were determined with a stop watch. With each flow meter, reproducibility was within about  $\pm 0.5\%$ .

Flow determinations were made with each of six convergent-divergent nozzles constructed from sapphire ring watch bearings (Moser Jewel Company, Perth Amboy, N.J.). Throat diameters were 0.0102, 0.0203, 0.0296, 0.0520, 0.0798, and 0.0941 in. The ratios of radius of curvature at the throat to nozzle throat radius were, respectively, 1.33, 2.18, 1.00, 0.83, 1.04, and 1.00. The nozzle diameters were determined with a Vickers projection microscope having an eyepiece reticule system carefully calibrated against a standard scale in the focal plane of the microscope. With a precision of  $\pm 0.0001$  in., diameters were measured at 45-deg intervals around the circumference. The effective geometric nozzle diameter was taken as the average of these eight measurements. With the smallest nozzle, the standard deviation from the arithmetic mean was 0.5% of the mean. The probable percentage error was  $\pm 0.4\%$ . Even smaller relative errors were encountered with the larger nozzles.

The radius of curvature at the throat was determined with a compass on photomicrographs of the nozzle wall profiles. In order to minimize distortion due to the high refractive index of sapphire, the nozzles were photographed while immersed in a drop of diiodomethane. It has a refractive index slightly lower than sapphire, 1.75 vs 1.76. As a typical example, the photomicrograph for the 0.0203-in. nozzle is shown in Fig. 2. Also shown schematically is the way in which this nozzle was cemented into a Plexiglas flange, its inlet walls having been faired into a 30-deg conical entrance section. The 0.0296-in. nozzle was fitted similarly with a 116-deg entrance section. The other four nozzles were cemented into flanges with no additional entrance sections.

Flow measurements were made with each nozzle using argon, helium, nitrogen, and hydrogen. Stagnation temperatures were within a few degrees of 300 K. Stagnation pressures ranged from 4 to 2200 Torr, corresponding to an overall Reynolds number range from 100 to 34,000. An error analysis indicated that for the results reported here the maximum uncertainty was  $\pm 2.0\%$  and occurred at the low end of the Reynolds number range. At the high end, the uncertainty was nearer  $\pm 1.0\%$ .

We carried out another series of tests at stagnation temperatures of 485 K. The stagnation chamber assembly was machined from brass and heated by resistance windings. Temperature was measured by means of two copper/constantan thermocouples, one in the nozzle wall and the other in the stagnation chamber gas. The entire assembly was mounted in a large vacuum tank maintained at  $10^{-3}$  Torr by a 16-in. jet booster pump (Stokes series 150) backed by three large

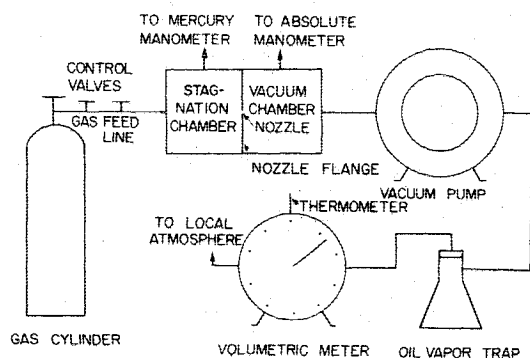


Fig. 1 Schematic of apparatus.

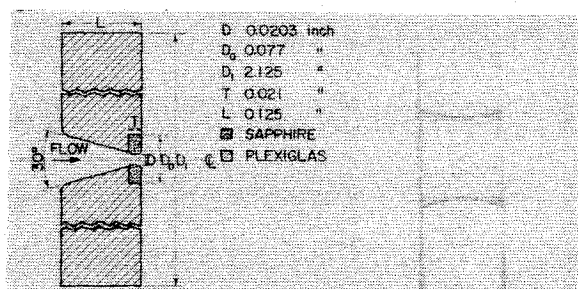


Fig. 2 Profile of the 0.0203-in. nozzle. The photomicrograph at right shows the throat region in detail.

mechanical pumps (one Kinney type 220 and two Stokes 412-H). The nozzle itself also was machined from brass. Its diameter, 0.0519 in., and radius of curvature, 0.0184 in., were determined from measurements on a photomicrograph of an epoxy resin plug made using the nozzle as a mold. A thin coat of oil prevented the cured resin from sticking. Because the nozzle was used at high temperature, a correction to the diameter of 0.8% due to thermal expansion was applied. Flow rates were determined using the previously calibrated 0.0203-in. nozzle as a meter. It was mounted outside the vacuum tank but in series with the heated nozzle. Both nozzles were choked at all times. Measurements were made with argon, helium, and nitrogen at stagnation pressures (for the heated nozzle) from 9 to 300 Torr. The corresponding Reynolds number range was from 160 to about 5000. At the highest Reynolds number, the overall error was about  $\pm 2.7\%$ . At the lowest, it was about  $\pm 3.6\%$ . We emphasize that these percentages represent maximum absolute uncertainties. Relative to the discharge coefficient for the metering nozzle, the errors are about half these values.

### III. Results and Discussion

The room-temperature results are shown in Figs. 3-6, one for each of the four gases. The high-temperature measurements are in Figs. 7 and 8. Ordinate values are discharge coefficients, the ratios of observed mass flow to the ideal isentropic mass flow based on measured stagnation conditions and nozzle diameters. Abscissas are in terms of the modified Reynolds number as defined by Eq. (2). The solid curve on each figure represents the theoretical value of the discharge coefficient calculated from Eq. (1), i.e., the analytical solution of the transformed governing equations based on a value of infinity for  $\beta$ , the pressure gradient parameter. The basis for the dashed curves will be set forth subsequently.

In view of the fact that no empirically adjustable parameters have been invoked, the agreement between theory and experiment is remarkable. Except for hydrogen, it is within experimental error (indicated by flags) down to

Reynolds numbers of about 500. In all cases, including hydrogen, the measured value of the discharge coefficient is slightly higher than the theory predicts. Even though it is small, let us examine the discrepancy.

First we note that the theoretical value of  $C_D$  presumes a value of infinity for the pressure gradient parameter  $\beta$ . The

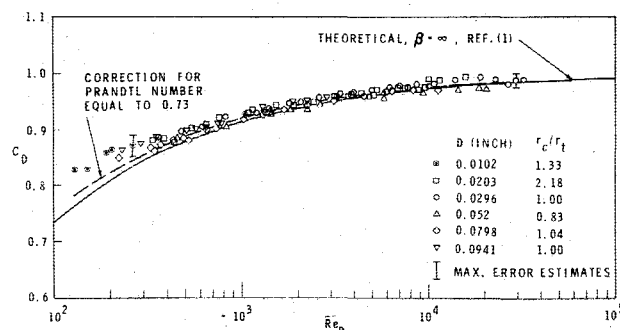


Fig. 5 Comparison of experimental and theoretical discharge coefficients for nitrogen with  $\gamma = 1.4$ .

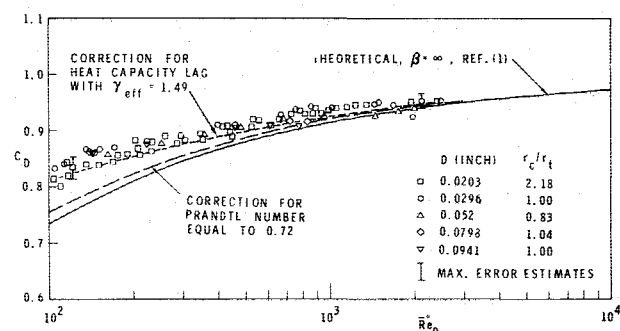


Fig. 6 Comparison of experimental and theoretical discharge coefficients for hydrogen with  $\gamma = 1.4$ .

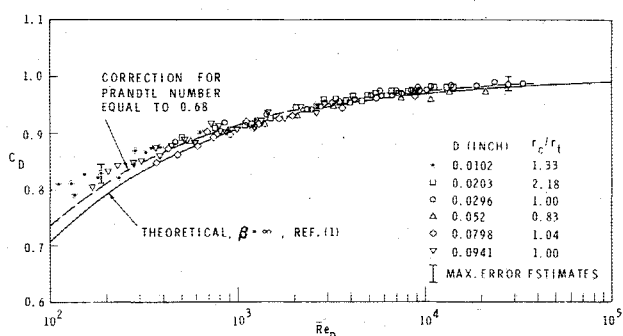


Fig. 3 Comparison of experimental and theoretical discharge coefficients for argon with  $\gamma = 1.67$ .

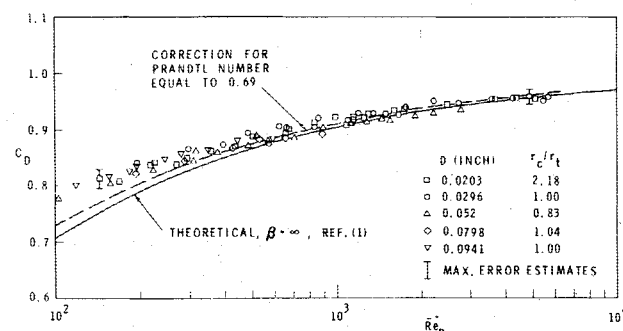


Fig. 4 Comparison of experimental and theoretical discharge coefficients for helium with  $\gamma = 1.67$ .

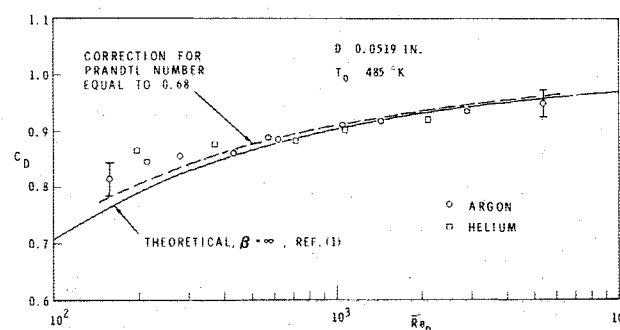


Fig. 7 Discharge coefficients for argon and helium in a heated nozzle with  $\gamma = 1.67$ .

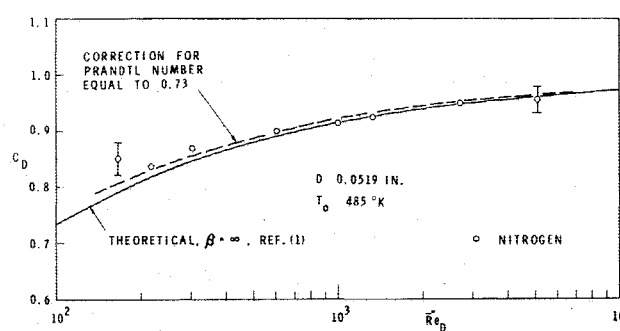


Fig. 8 Discharge coefficients for nitrogen in a heated nozzle with  $\gamma = 1.4$ .

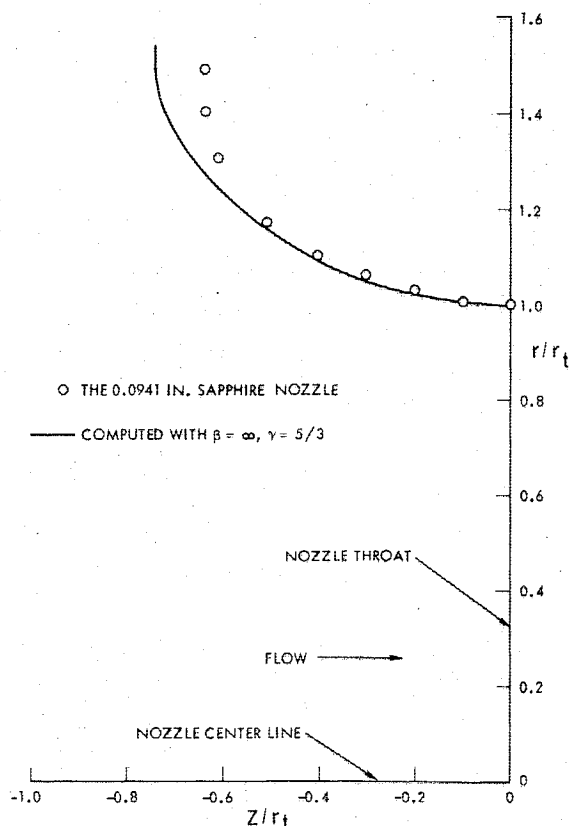


Fig. 9 An experimental nozzle contour compared with theoretical inviscid contour for  $r_c/r_t = 1.0$ .

numerical solutions of the equations for  $\beta=2$  and  $\beta=1$  showed slightly higher values for  $C_D$ . In fact, the theoretical curve for  $\beta=1$  matches the experimental points within the probable error down to Reynolds numbers of about 100. The question arises as to whether a value of unity for  $\beta$  might reflect more accurately the actual axial pressure gradient in the experiments. This possibility is not particularly tempting from a practical point of view, because it would require a numerical solution for each particular case in which it might be desired to predict a discharge coefficient. More important is the fact that a value of unity for  $\beta$  is not consistent with actual nozzle geometries. In Fig. 9 are shown what we have called "inviscid nozzle contours" for  $\beta=\infty$ . These contours are those that would provide in inviscid flow the axial pressure gradient corresponding to the associated value of  $\beta$ . They are based on the isentropic Mach number/area relations. In a real flow situation, these contours should relate roughly to the edge of the boundary layer, i.e., at the displacement thickness from the wall. Also shown in Fig. 9 as a fairly typical example is the actual contour of one of the nozzles that we used. After allowance for a boundary layer, it becomes clear that  $\beta=\infty$  is by far the best approximation. We must look elsewhere for an explanation of the difference between theory and experiment.

Another of the assumptions in the theory was that the flow was one-dimensional; i.e., the Mach number 1 surface is a plane at the nozzle throat except in the relatively thin boundary-layer region. It is well known, of course, that the velocity distribution in real nozzles is not uniform at any cross section. On the other hand, the one-dimensional approximation has been so useful and so successful in so many situations that one questions it with some reluctance, especially in a situation that should be fairly insensitive to a small departures from uniformity of velocity distribution. Moreover, the product of density and velocity per unit area is maximum at Mach number 1. Any variation from sonic velocity in the plane of the throat should result in a decrease in actual mass flow and, therefore, a decrease in the ex-

perimental  $C_D$  relative to one-dimensional theory. Departures from one-dimensionality thus do not seem capable of explaining apparent increase in discharge coefficient relative to theory.

A further and usual assumption in the analysis was a Prandtl number of unity. For the gases that we used, the actual Prandtl numbers are in the range from 0.68 to 0.73. One consequence of Prandtl number less than unity is that the wall recovery temperature is less than the freestream stagnation temperature. In our nozzles, the thermal capacity and conductivity are fairly large, so that the wall temperature might have been higher than the recovery temperature. The resulting heat transfer to the gas would undermine the assumption of an adiabatic wall. Addition of heat to the gas would bring about a decrease in mass flow in an amount approximately proportional to the square root of the resulting temperature rise, averaged over all of the gas. This temperature rise must have been tiny, if it existed at all. Thus, the effect of heat transfer is not only small but is in the wrong direction to explain the observed discrepancy.

However, a decrease in recovery temperature consequent to Prandtl numbers less than unity would cause a decrease in viscosity near the wall. Clearly, an increase in mass flow would result, and this effect is in the right direction. It would be difficult to solve the equations for values of Prandtl number less than unity. Nevertheless, we can estimate the effect of Prandtl number by noting that the most important consequence of viscosity is at the wall. It would seem appropriate, therefore, to compute the Reynolds number for each experimental mass flow point by using a value of viscosity relevant to the actual temperature at the wall rather than to a wall temperature that would result from assuming a Prandtl number of unity. In our procedure, this relevance would be achieved by using recovery temperature rather than stagnation temperature as the basis for computing freestream viscosity. We estimate that this correction amounts to an increase of about 4% in the Reynolds number to be associated with each experimental point in Figs. 3-8. The net effect would be to shift each point slightly to the right.

The decrease in wall temperature due to Prandtl number less than unity also would cause a slight increase in the theoretical value of  $C_D$ . Recall that the product of velocity and density for the gas,  $\rho u$ , increases with the square root of temperature. We estimate that this effect would result in an increase in the theoretical values of  $C_D$  of about 1% in the Reynolds number range below 1000. As the boundary layer gets thinner at high Reynolds numbers, the effect becomes smaller. The net effect of this correction is to raise the theoretical curve slightly at the lower end.

We find that the overall consequence of these two estimated corrections can be allowed for empirically by the simple expedient of dividing the Reynolds number computed for each point by the square root of the Prandtl number. The equivalent representation of this effect in the drawings would be to shift the theoretical curve to the left. The dashed curve in each figure shows such a shift in the theoretical curve. The correction brings agreement (within experimental error) between theory and measurement down to Reynolds numbers of about 200, again excepting hydrogen.

Even after the correction for Prandtl number, there remains a consistent excess in the measured values of  $C_D$  at the low end of the Reynolds number range. In our view, this excess represents the onset of slip effects, which would invalidate the boundary-layer assumption of zero velocity at the wall. In the limit of very low stagnation pressure, the actual mass flow will approach the free molecule effusive limit. At this limit  $C_D$ , as we have defined it, will have a value of the order of 0.5 for reasonable values of  $\gamma$  and nozzle shape (Clausius factor). This limiting value will be reached when the mean free path in the source gas is of the same order as the nozzle diameter, i.e., at a value of about unity for the Reynolds number as we have defined it. Clearly the theory,

which can be expected to be valid only at relatively high Reynolds numbers, must break down long before this lower limit corresponding to effusive flow. In general, we should expect slip effects to become appreciable when the mean free path becomes an appreciable fraction of the boundary-layer thickness. For our situation, the ratio of mean free path to boundary-layer thickness is given approximately by

$$\frac{\lambda}{\delta^*} = \frac{2}{Re_D^*(1 - \sqrt{C_D})} \quad (3)$$

where  $\lambda$  is the mean free path and  $\delta^*$  is the boundary-layer displacement thickness. At a Reynolds number of 200, this ratio already has the appreciable value of 0.05, and so we should expect that slip effects should have started to intrude as, indeed, they seem to have done.

There remains the problem of explaining why the results for hydrogen are consistently higher than for the other gases. We recall that, in comparison with nitrogen and other molecules, hydrogen has a relatively low rate of energy exchange between translation and rotation.<sup>24-26</sup> This so-called rotational relaxation rate can be characterized by the number of collisions required for the average hydrogen molecule to lose  $(e-1)/e$  of its excess rotational energy, i.e., to reduce the difference between rotational temperature and translational temperature to  $1/e$  of its original value in a system not at thermal equilibrium. This characteristic collision number for nitrogen is about 5. For hydrogen it is about 300. Thus, we should expect that departures from equilibrium would be much more likely with hydrogen. During a recent study of rotational relaxation, Gallagher carried out some numerical calculations on relaxation effects in the flow upstream of the throat in small sonic nozzles.<sup>25</sup> He found that the extent of the relaxation was not very dependent upon nozzle contour, probably for the same reasons that discharge coefficient also is fairly insensitive to the pressure gradient parameter. In a typical case for hydrogen with  $T_0 = 300$  K and  $P_0 = 200$  Torr in a nozzle of 0.010 in. diam, he found that  $T_{rot}$  at the throat was  $0.89 T_0$ , appreciably higher than the equilibrium value of  $0.833 T_0$ . If the rotation had not relaxed at all, the effective value of  $\gamma$  would have been  $5/3$ , and the rotational temperature would have remained at  $T_0$ . If we make a linear interpolation, we find an actual effective value of  $\gamma$  equal to about 1.49 for hydrogen under these conditions, which correspond to a Reynolds number of 524.

According to Eq. (1), it turns out that there is a very small dependence of  $C_D$  upon the specific heat ratio. At first glance, therefore, it might be thought that heat capacity lags could be neglected. Actually, it is in the computation of the reference isentropic mass flow that the effect becomes significant, although still rather small. The isentropic mass flow for  $\gamma = 5/3$  is only about 6.4% higher than for  $\gamma = 7/5$ , other things being equal. Thus, the increase in the effective value of  $\gamma$  from 1.4 to 1.49 in the preceding example would increase the isentropic mass flow by about 4%. This increase would correspond to decreasing the experimental value of  $C_D$  in Fig. 6 by about 4% at Reynolds numbers near 500. We have extended these calculations and represented the result of incomplete relaxation by an equivalent increase in the theoretical value of  $C_D$  for hydrogen. The result is shown as a dotted line in Fig. 6. Clearly, the heat capacity lag seems capable of explaining most of hydrogen's excessive discrepancy between theory and experiment relative to the other gases. The important point is that one should be alert to the fact that departures from equilibrium can be significant at low Reynolds numbers. In particular, the characteristic collision numbers for vibrational relaxation rates and chemical reaction rates are generally very much larger than for rotational relaxation in hydrogen. Much greater deviations in  $C_D$  can be expected from heat capacity lags due to these effects.

#### IV. Conclusions

The rather remarkable agreement between the experimental and theoretical values for discharge coefficients suggests that a priori predictions by Eq. (1) can be accurate to at least within our experimental error of about 2%. Unless extreme precautions are taken in measurement, the theoretically predicted values are probably more reliable than values obtained by experimental calibration. Certainly they are easier to obtain. Of course, there are also precautions to be observed in using Eq. (1). We summarize here the important ones:

1) Experimental confirmation with respect to the effect of radius of curvature has been limited to values of  $r_c/r_t$  between 0.71 and 2.18. We should expect no difficulties in modest extensions of this range.

2) The Reynolds number to be inserted in Eq. (1) is defined as

$$\overline{Re}_D^* = (\rho_e u_e D / \mu_e) * (r_c Pr / r_t)^{-1/2}$$

where  $\rho_e$ ,  $u_e$ , and  $\mu_e$  are freestream values of density, velocity, and viscosity, an asterisk indicates Mach number 1, and  $Pr$  is the Prandtl number. (The presence of Prandtl number has only empirical justification.)

3) Experimental confirmation has been limited to heat capacity ratios of  $5/3$  and  $7/5$ . We expect equivalent validity with other values of  $\gamma$  provided that equilibrium is maintained. At low Reynolds numbers, departures from thermal and chemical equilibrium can cause errors.

4) In the absence of departures from equilibrium, Eq. (1) can be relied upon at Reynolds numbers greater than about 200. At lower values, slip and rarefaction effects become important.

#### Acknowledgment

Support for this research was provided in part by the National Science Foundation under Grant GK 655 and in part from the Office of Naval Research under Project SQUID, Contract No. 3623 (NR-098-038). We also are very grateful for the assistance of our colleagues at Princeton, J. B. Anderson, R. P. Andres, J. Bittner, and D. G. H. Marsden.

#### References

- Tang, S., "Discharge Coefficients for Critical Flow Nozzles and Their Dependence on Reynolds Numbers," Ph.D. Thesis, Princeton Univ., 1969.
- Simmons, F. S., "Analytical Determination of the Discharge Coefficients of Flow Nozzles," NACA TN 3447, 1955.
- Rivas, M. A. and Shapiro, A. H., "On the Theory of Discharge Coefficients for Rounded-Entrance Flowmeters and Venturis," *Transactions of ASME*, Vol. 78, April 1956, pp. 489-497.
- Back, L. H., Massier, P. F., and Gier, H. L., "Comparison of Measured and Predicted Flows Through Conical Supersonic Nozzles, With Emphasis on the Transonic Region," *AIAA Journal*, Vol. 3, Sept. 1965, pp. 1606-1614.
- Arnberg, B. T., "Review of Critical Flowmeters for Gas Flow Measurements," *Journal of Basic Engineering*, Vol. 84, American Society of Mechanical Engineers Paper 61-WA-181, Dec. 1961, pp. 447-460.
- Smetana, F. O., "Convergent-Divergent Nozzle Discharge Characteristics in the Transition Regime Between Free Molecule and Continuum Flow," American Society of Mechanical Engineers Paper 63-WA-94, Jan. 1964.
- Milligan, M. W., "Nozzle Characteristics in the Transition Regime Between Continuum and Free Molecular Flow," *AIAA Journal*, Vol. 2, June 1964, pp. 1088-1092.
- Hall, I. M., "Transonic Flow in Two-Dimensional and Axially-Symmetric Nozzles," *Quarterly Journal of Mechanics and Applied Mathematics*, Vol. XV, Pt. 4, Nov. 1962, pp. 487-508.
- Back, L. H. and Witte, A. B., "Prediction of Heat Transfer from Laminar Boundary Layers, With Emphasis on Large Free-Stream Velocity Gradients and Highly Cooled Walls," *Journal of Heat Transfer*, Vol. 88, Aug. 1966, pp. 249-256.

<sup>10</sup>Massier, P. F., Back, L. H., Noel, M. B., and Saheli, F., "Viscous Effects on the Flow Coefficient for a Supersonic Nozzle," *AIAA Journal*, Vol. 8, March 1970, pp. 605-607.

<sup>11</sup>Back, L. H., "Acceleration and Cooling Effects in Laminar Boundary Layers—Subsonic, Transonic, and Supersonic Speeds," *AIAA Journal*, Vol. 8, April 1970, pp. 794-802.

<sup>12</sup>Back, L. H. and Cuffel, R. F., "Relationship Between Temperature and Velocity Profiles in a Turbulent Boundary Layer Along a Supersonic Nozzle with Heat Transfer," *AIAA Journal*, Vol. 8, Nov. 1970, pp. 2066-2069.

<sup>13</sup>Back, L. H. and Cuffel, R. F., "Flow Coefficients for Supersonic Nozzles with Comparatively Small Radius of Curvature Throats," *Journal of Spacecraft and Rockets*, Vol. 8, Feb. 1971, pp. 196-198.

<sup>14</sup>Kuluva, N. M. and Hosack, G. A., "Supersonic Nozzle Discharge Coefficients at Low Reynolds Numbers," *AIAA Journal*, Vol. 9, Sept. 1971, pp. 1876-1879.

<sup>15</sup>Rothe, D. E., "Electron-Beam Studies of Viscous Flow in Supersonic Nozzles," *AIAA Journal*, Vol. 9, May 1971, pp. 804-810.

<sup>16</sup>Rac, W. J., "Some Numerical Results on Viscous Low-Density Nozzle Flows in the Slender-Channel Approximation," *AIAA Journal*, Vol. 9, May 1971, pp. 811-820.

<sup>17</sup>Back, L. H., Cuffel, R. F., and Massier, P. F., "Influence of Contraction Section Shape and Inlet Flow Direction on Supersonic Nozzle Flow and Performance," *Journal of Spacecraft and Rockets*, Vol. 9, June 1972, pp. 420-427.

<sup>18</sup>Potter, J. L. and Carden, W. H., "Design of Axisymmetric Contoured Nozzles for Laminar Hypersonic Flow," *Journal of Spacecraft and Rockets*, Vol. 5, Sept. 1968, pp. 1095-1100.

<sup>19</sup>Back, L. H., "Transonic Laminar Boundary Layers with Surface Curvature," *International Journal of Heat and Mass Transfer*, Vol. 16, Sept. 1973, pp. 1745-1761.

<sup>20</sup>Olson, A. T., "Nozzle Discharge Coefficient—Compressible Flow," *Journal of Fluids Engineering*, Vol. 96, March 1974, pp. 21-24.

<sup>21</sup>Cline, M. C., "Computation of Two-Dimensional, Viscous Nozzle Flow," *AIAA Journal*, Vol. 14, March 1976, pp. 295-296.

<sup>22</sup>Back, L. H. and Cuffel, R. F., "Compressible Laminar Boundary Layers with Large Acceleration and Cooling," *AIAA Journal*, Vol. 14, July 1976, pp. 968-971.

<sup>23</sup>Edwards, R. H., "Low-Density Flows through Tubes and Nozzles," *AIAA Progress in Astronautics and Aeronautics: Rarefied Gas Dynamics*; edited by J. L. Potter, Vol. 51, Pt. I, AIAA, New York, 1977, pp. 199-223.

<sup>24</sup>Herzfeld, K. and Litovitz, T., *Absorption and Dispersion of Ultrasonic Waves*, Academic Press, New York, 1959.

<sup>25</sup>Gallagher, R. J. and Fenn, J. B., "Rotational Relaxation of Molecular Hydrogen," *Journal of Chemical Physics*, Vol. 60, May 1974, p. 3492.

<sup>26</sup>Gallagher, R. J., "Internal Energy Relaxation in Gases," Ph.D. Thesis, Yale Univ., 1972.

## *From the AIAA Progress in Astronautics and Aeronautics Series...*

### **EXPERIMENTAL DIAGNOSTICS IN GAS PHASE COMBUSTION SYSTEMS—v. 53**

*Editor: Ben T. Zinn; Associate Editors: Craig T. Bowman,  
Daniel L. Hartley, Edward W. Price, and James F. Skiffstad*

Our scientific understanding of combustion systems has progressed in the past only as rapidly as penetrating experimental techniques were discovered to clarify the details of the elemental processes of such systems. Prior to 1950, existing understanding about the nature of flame and combustion systems centered in the field of chemical kinetics and thermodynamics. This situation is not surprising since the relatively advanced states of these areas could be directly related to earlier developments by chemists in experimental chemical kinetics. However, modern problems in combustion are not simple ones, and they involve much more than chemistry. The important problems of today often involve nonsteady phenomena, diffusional processes among initially unmixed reactants, and heterogeneous solid-liquid-gas reactions. To clarify the innermost details of such complex systems required the development of new experimental tools. Advances in the development of novel methods have been made steadily during the twenty-five years since 1950, based in large measure on fortuitous advances in the physical sciences occurring at the same time. The diagnostic methods described in this volume—and the methods to be presented in a second volume on combustion experimentation now in preparation—were largely undeveloped a decade ago. These powerful methods make possible a far deeper understanding of the complex processes of combustion than we had thought possible only a short time ago. This book has been planned as a means of disseminating to a wide audience of research and development engineers the techniques that had heretofore been known mainly to specialists.

671 pp., 6x9, illus., \$20.00 Member \$37.00 List

TO ORDER WRITE: Publications Dept., AIAA, 1290 Avenue of the Americas, New York, N.Y. 10019